Supplementary information

Supplementary information relative to the manuscript titled “Limited effect of basalt amendment and mycorrhizal inoculation on soil chemical properties and maize growth on a nutrient-rich soil”

Lucilla Boito, Jet Rijnders, Laura Steinwidder, Patrick Frings, Arthur Vienne, Mirthe Maes, Erik Verbruggen, and Sara Vicca

S1: Estimation of theoretical (laboratory-based) weathering rates of the amended feedstock.

Theoretical weathering rates were estimated from the feedstock's mineralogical and elemental composition (determined by XRD and XRF) using dissolution rate laws from Palandri and Kharaka (2004) for crystalline silicates and calcite, and from Gislason and Oelkers (2003) for basaltic glass. Rates were estimated at 21 °C using the range of porewater pH values measured in this study. For basaltic glass, dissolved Al concentrations were additionally incorporated into the rate calculations following Gislason and Oelkers (2003; Equation 13 in their text). The overall basalt weathering rate was then calculated as the mass-fraction-weighted sum of the charge-equivalent dissolution fluxes of the individual mineral phases.

Supplementary Figures

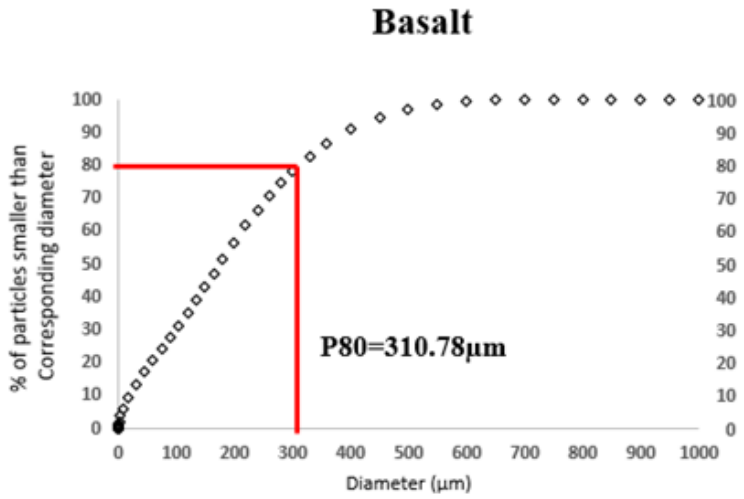


Figure S1: Particle size distribution of basalt. P80= 80% of the particles have a diameter less than or equal to this size.

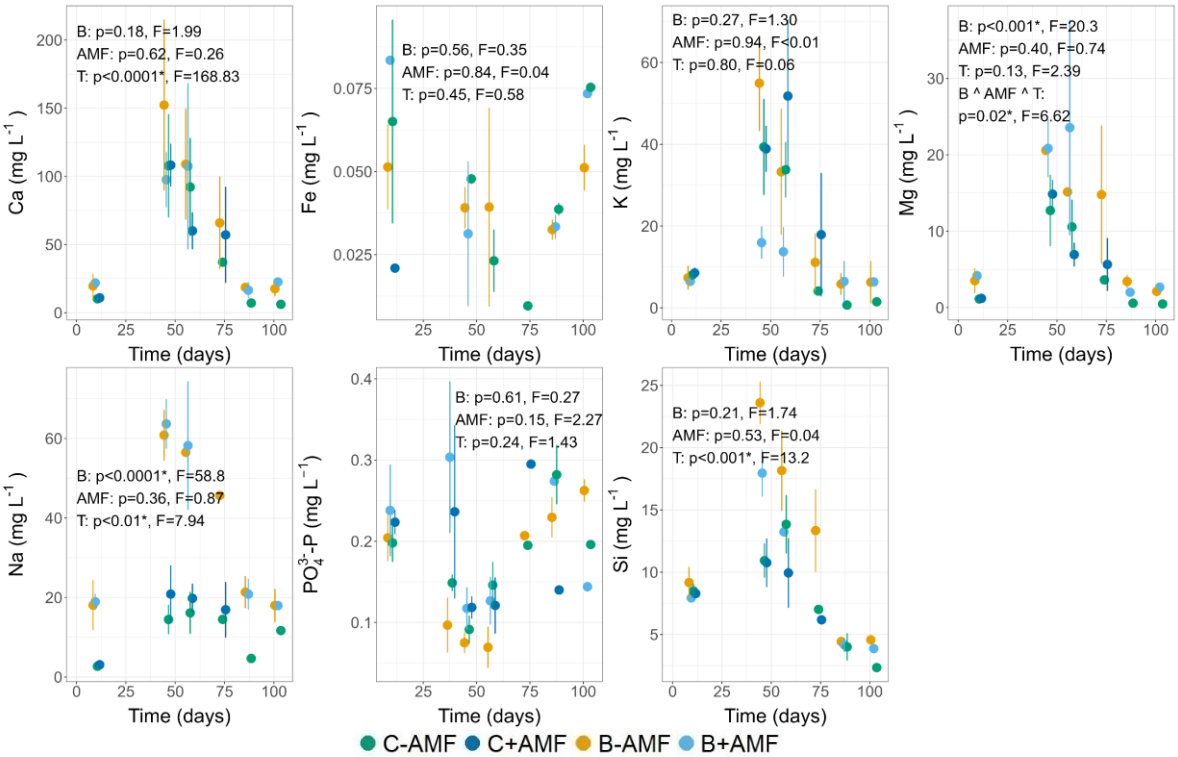


Figure S2: Mean concentrations of elements and nutrients in the pore water (Ca, Fe, K, Mg, Na, PO_4^{3-}-P and Si) during the experiment for the four treatments (C-AMF = control without AMF, C+AMF = control with AMF, B-AMF = basalt without AMF, B+AMF = basalt with AMF). Error bars represent the standard error on the mean. p- and F-values are shown from a linear regression analysis with element or nutrient concentration as response variable and basalt (B), AMF and time (T), and their relevant interactions, as covariables. When interactions were not significant, they were excluded from the model and not shown here. Interactions are indicated by carets (^), while significant relationships by an asterisk (*).

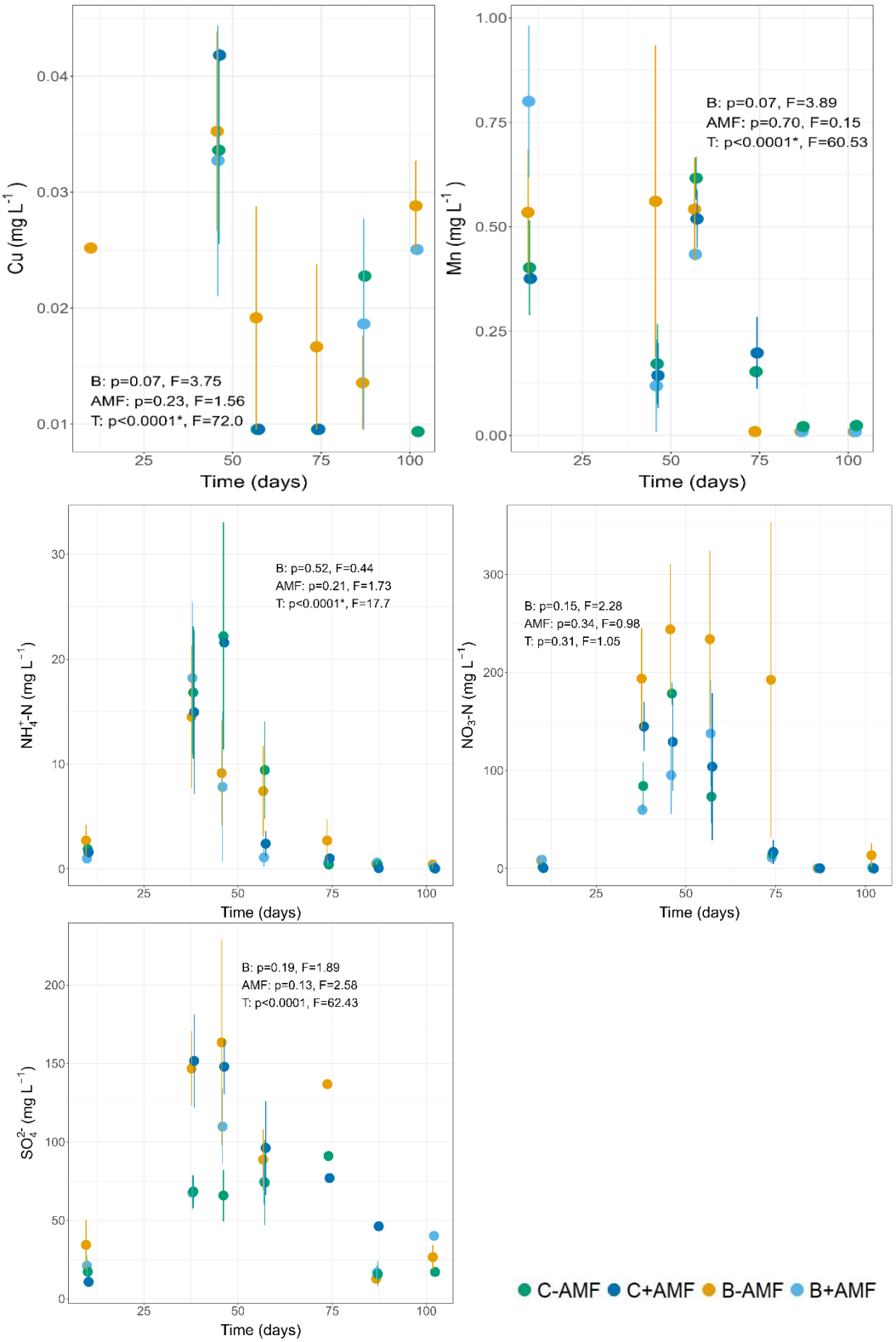


Figure S3: Mean concentrations of copper (Cu), manganese (Mn), ammonium-nitrogen (NH_4^+-N), nitrate-nitrogen (NO_3^--N) and sulphate (SO_4^{2-}) in the pore water during the experiment for the four treatments (C-AMF = control without AMF, C+AMF = control with AMF, B-AMF = basalt without AMF, B+AMF = basalt with AMF). Error bars represent the standard error on the mean. p- and F-values are shown from a linear regression analysis with element or nutrient concentration as response variables and basalt (B), AMF and time (T), and their relevant interactions, as covariables. When interactions were not significant, they were excluded from the model and not shown here. Interactions are indicated by carets (^), while significant relationships by an asterisk (*).

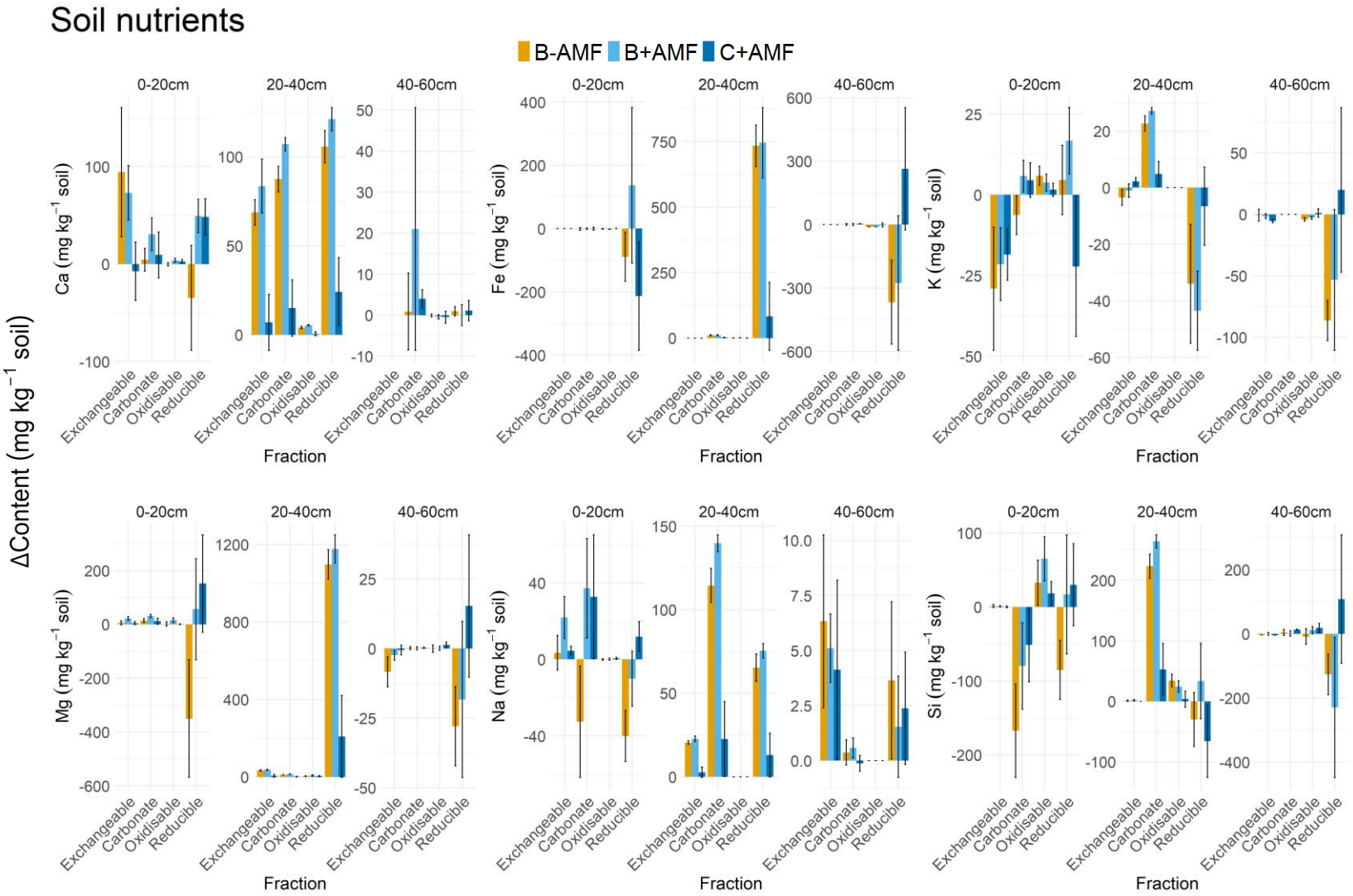


Figure S4: Mean soil nutrient Δ contents (Ca, Fe, K, Mg, Na and Si) for the three treatments (B-AMF = basalt without AMF, B+AMF = basalt with AMF, C+AMF = control with AMF) at the end of the growing season. Nutrient concentrations are shown as the difference between the start and the end of the growing season, and are shown compared to the control treatment (control without AMF). Soils were divided into three sampling depths (0-20 cm, 20-40 cm, 40-60 cm) for which nutrient concentrations were measured in four soil fractions (exchangeable, carbonate, oxidisable and reducible fraction) with sequential extraction analysis according to Tessier et al (1979).

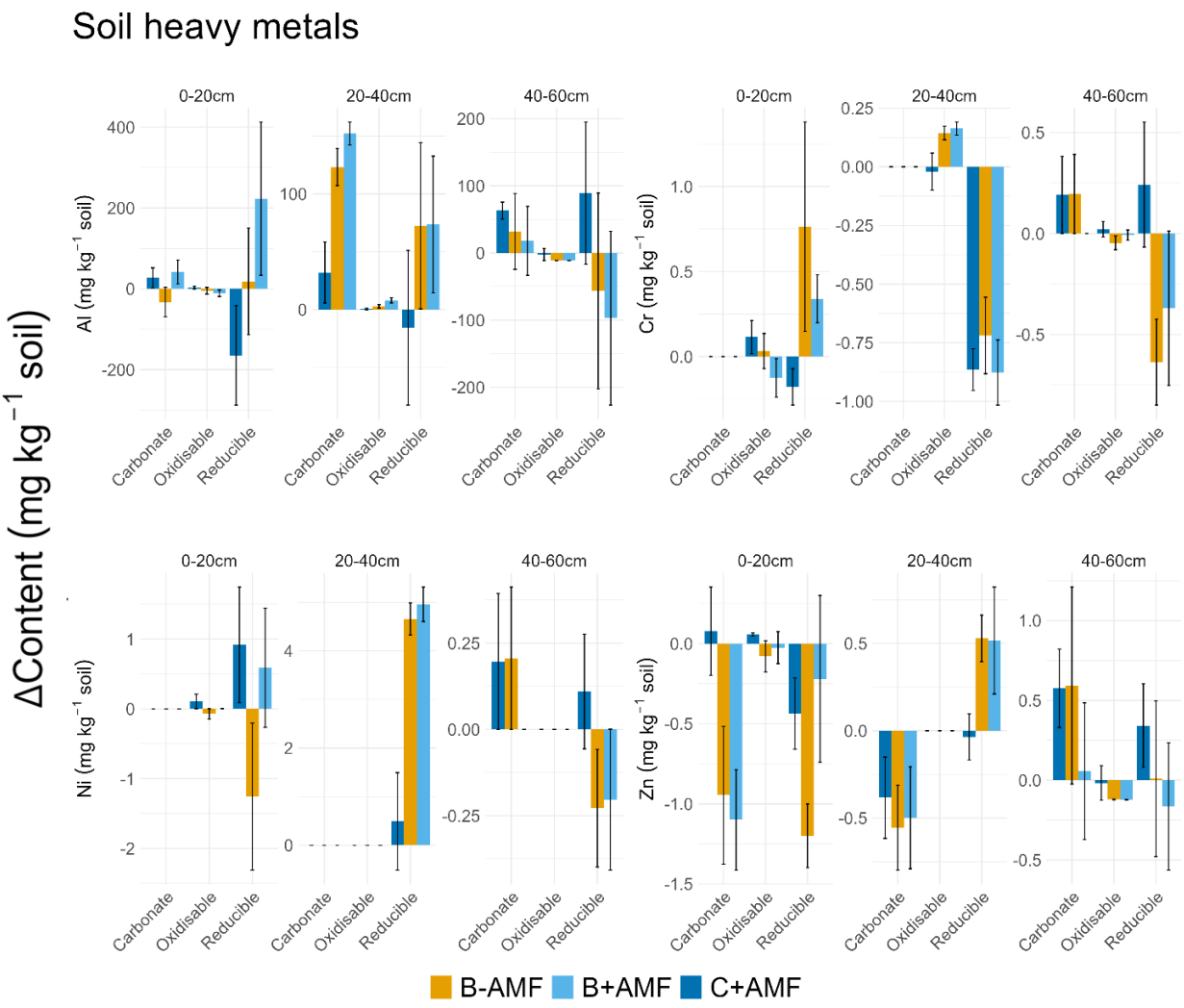


Figure S5: Mean soil heavy metal (Al, Cr, Ni and Zn) Δ content for the three treatments (B-AMF = basalt without AMF, B+AMF = basalt with AMF, C+AMF = control with AMF) at the end of the growing season. Concentrations are shown as the difference between the start and the end of the growing season, and are shown compared to the control treatment (C-AMF = control without AMF). Soils were divided into three sampling depths (0-20 cm, 20-40 cm, 40-60 cm) for which nutrient contents were measured in four soil fractions (exchangeable, carbonate, oxidizable and reducible fraction) with sequential extraction method after Tessier et al. (1979).

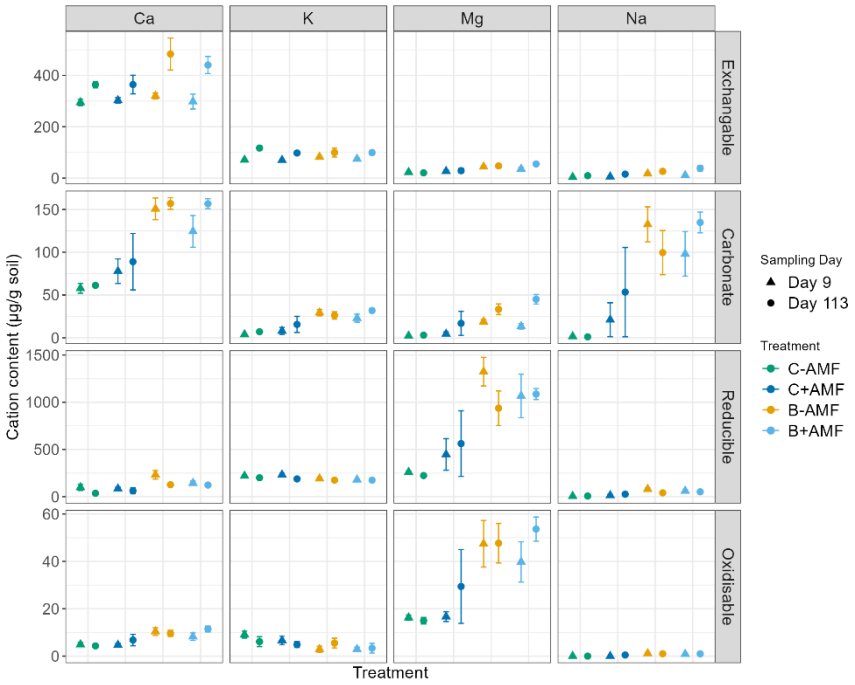


Figure S6: average Ca, K, Mg and Na content in the four sequentially extracted soil pools at day 9 (triangles) and 113 (circles) for each treatment (B-AMF = basalt without AMF, B+AMF = basalt with AMF, C+AMF = control with AMF). Error bars represent the standard error on the mean. Vey small error bars are not visible due to overlap with data points.

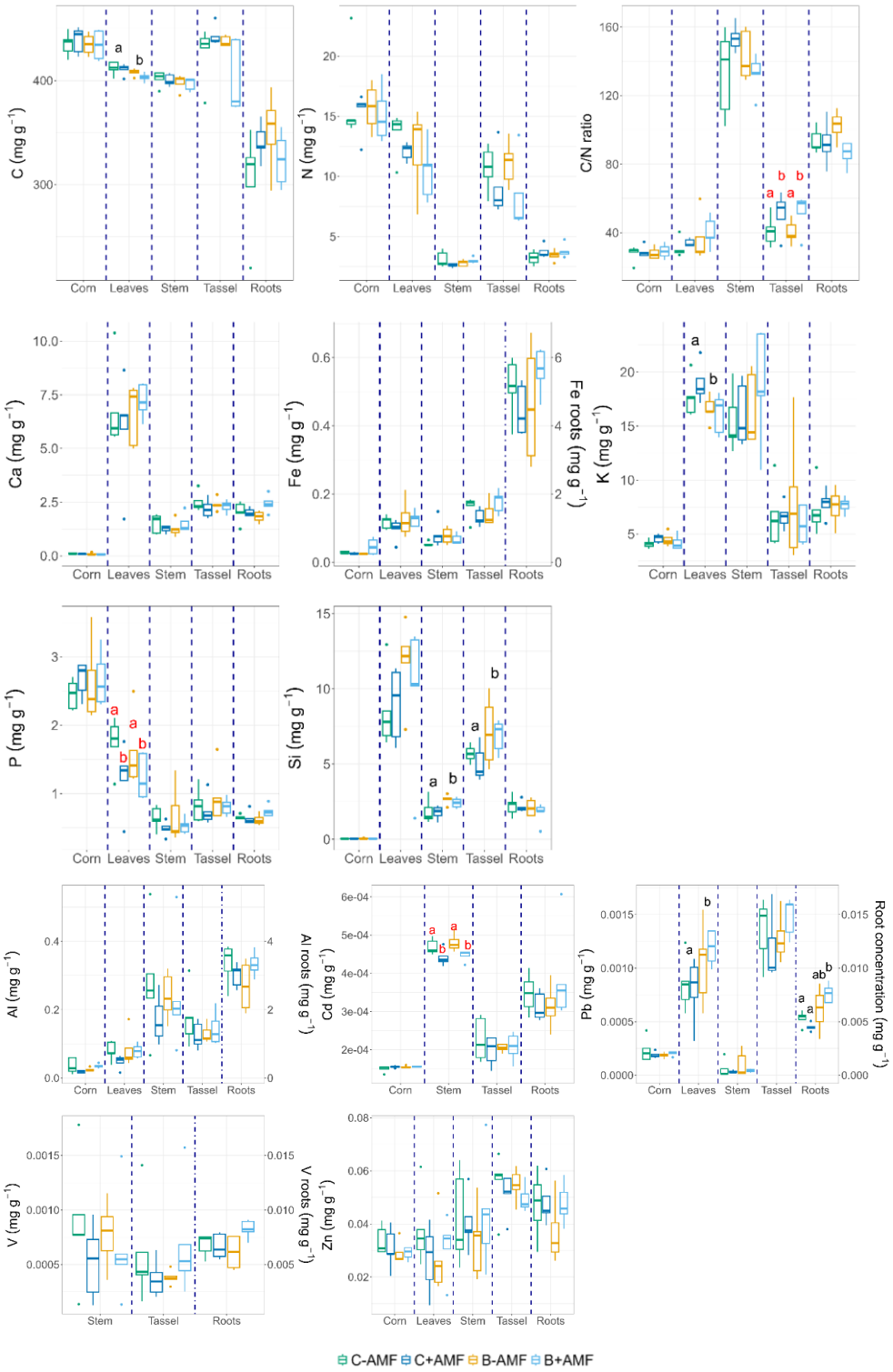


Figure S7: C, N, C/N ratio, Ca, Fe, K, P, Si, Al, Cd, Pb, V and Zn contents in the corn, leaves, stem, tassel, and roots for the four treatments (C-AMF = control without AMF, C+AMF = control with AMF, B-AMF = basalt without AMF, B+AMF = basalt with AMF). C and N contents were determined by dry combustion based on the Dumas method using an elemental analyser (FLASH 2000, Interscience, Louvain-la-Neuve, Belgium). For each plant sample, 0.3 g was weighed and digested with HNO_3 and H_2O_2. Corn and leaf V concentrations were all below the limit of quantification (<0.0001 mg g^{-1}) and are therefore not presented. Boxes represent the interquartile range (25th-75th percentile), horizontal lines indicate the median, and whiskers extend to the most extreme data points within 1.5x of the interquartile range. Points outside this range are plotted as outliers. Note that for Al, Cd, Fe, Pb and V, the primary axis shows the content in the corn, leaves, stems, and tassels while the secondary axis shows the content in the roots. p- and F-values are shown in Table S19. Significant differences are indicated with a different letter, while a similar letter means no differences between those treatments. Black letters indicate basalt effects, while red letter indicate AMF effects. If no letters are shown for a combination of plant part and element, this means that there was no significant influence of basalt or AMF.

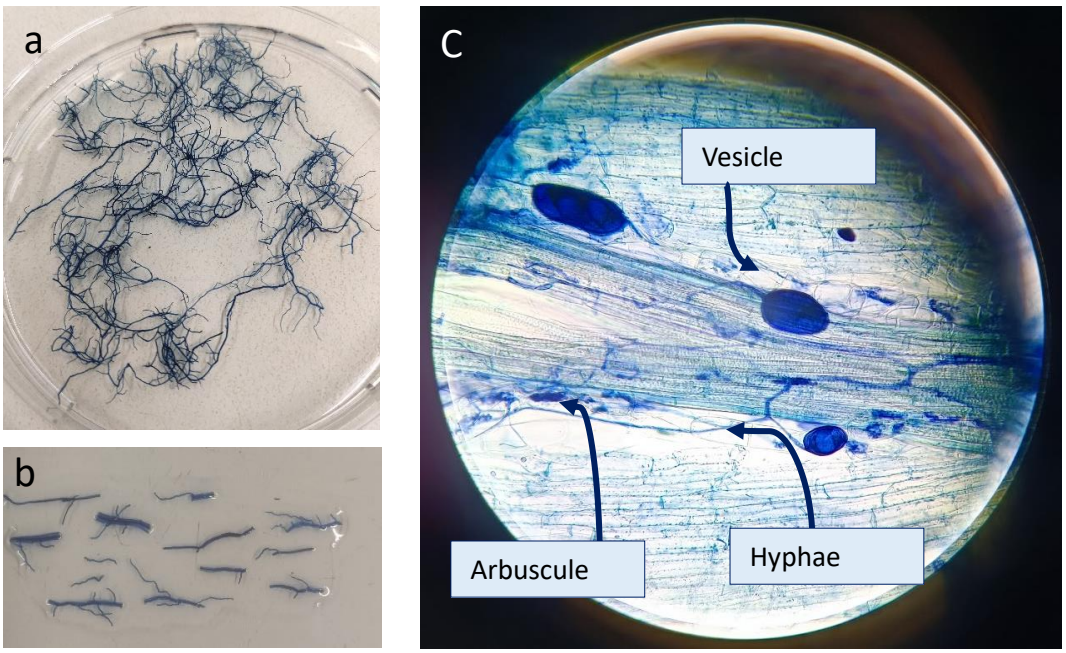


Figure S8: Overview of AMF colonization analysis. a) Roots stained with 10% Shaeffer Black ink in 10% acetic acid b) Slide with stained roots, c) Root under microscope with vesicles, arbuscules and hyphae.

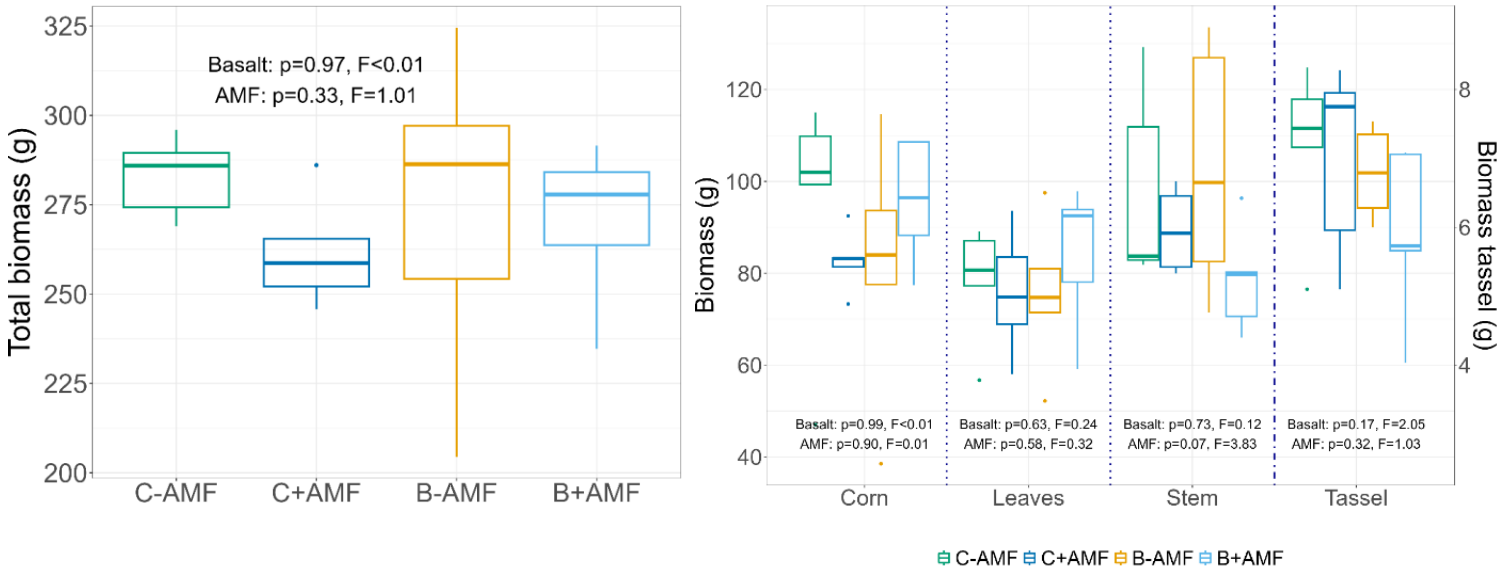


Figure S9: Total aboveground dry biomass (left) and aboveground biomass for each plant organ (right) determined after drying at 70 °C until constant weight for the four treatments (B-AMF = basalt without AMF, B+AMF = basalt with AMF, CP-A = control without AMF, CP+A = control with AMF) at the end of the experiment. Boxes represent the interquartile range (25th–75th percentile), horizontal lines indicate the median, and whiskers extend to the most extreme data points within 1.5× of the interquartile range. Points outside this range are plotted as outliers. p- and F-values from an ANOVA analysis with dry tissue biomass as response variables and basalt, AMF and their interaction as covariables are shown. Interactions were not significant and were excluded from the model. Significant relationships are indicated by an asterisk (*).

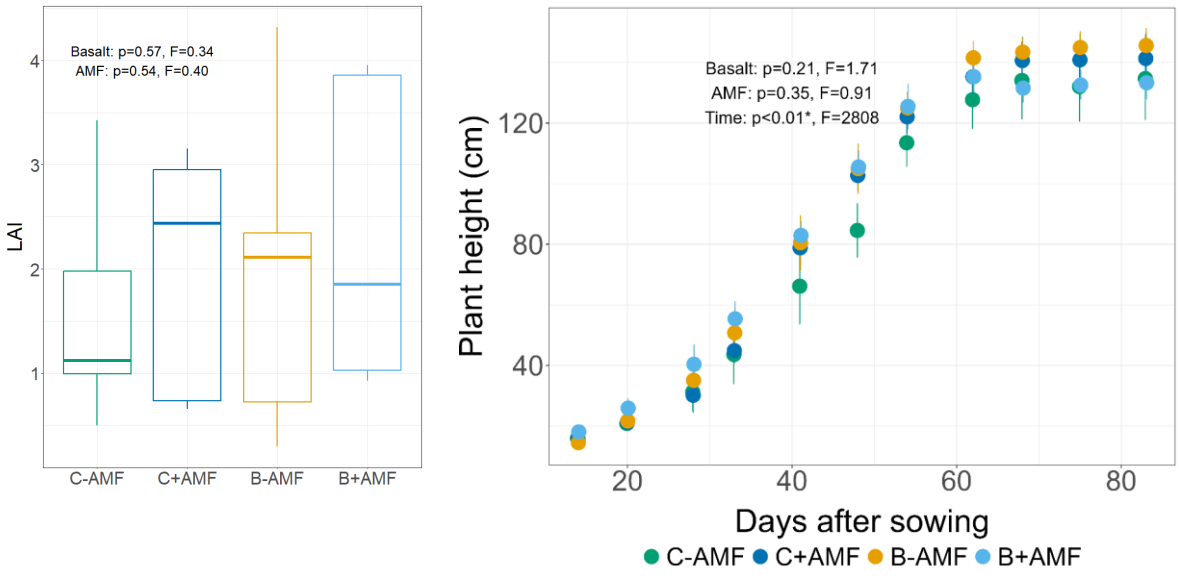


Figure S10: Leaf area index (LAI; left panel) in the middle of the growing season (20 July 2022) for each treatment (B-AMF = basalt without AMF, B+AMF = basalt with AMF, CP-A = control without AMF, CP+A = control with AMF), determined following Ven et al. (2019). Plant height during the experiment for each treatment (right panel). Left panel: p- and F-values are shown from an ANOVA analysis with LAI as response variable and basalt, AMF, and their interaction as covariables. The interaction was not significant and was excluded from the model. Significant relationships are indicated by an asterisk (*). Right panel: p- and F-values are shown from a regression analysis with plant height as fixed effect and basalt, AMF, time and their interaction as covariables. Interactions were not significant and were excluded from the model.

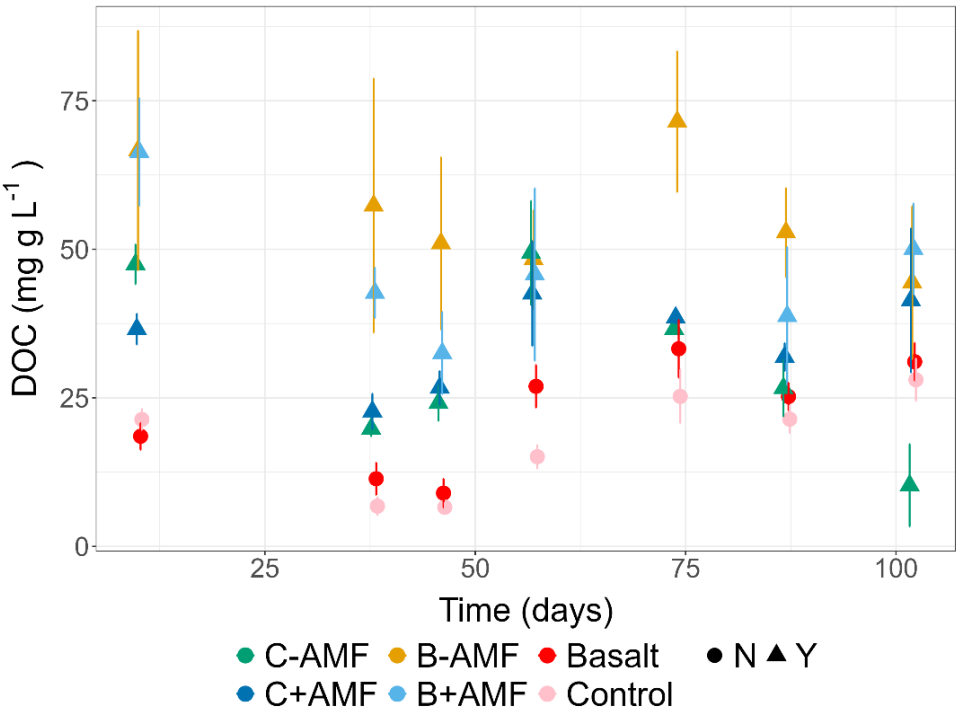


Figure S11: Mean dissolved organic carbon (DOC) concentration in the pore water over the experimental period in the four treatments which used pasteurized soil (B-AMF = basalt without AMF, B+AMF = basalt with AMF, CP-A = control without AMF, CP+A = control with AMF) compared to a parallel mesocosm experiment at the same location which used the same basalt and soil, without pasteurization. Pasteurized treatments are indicated by a triangle, unpasteurized ones by a circle. Error bars represent standard errors on the mean.

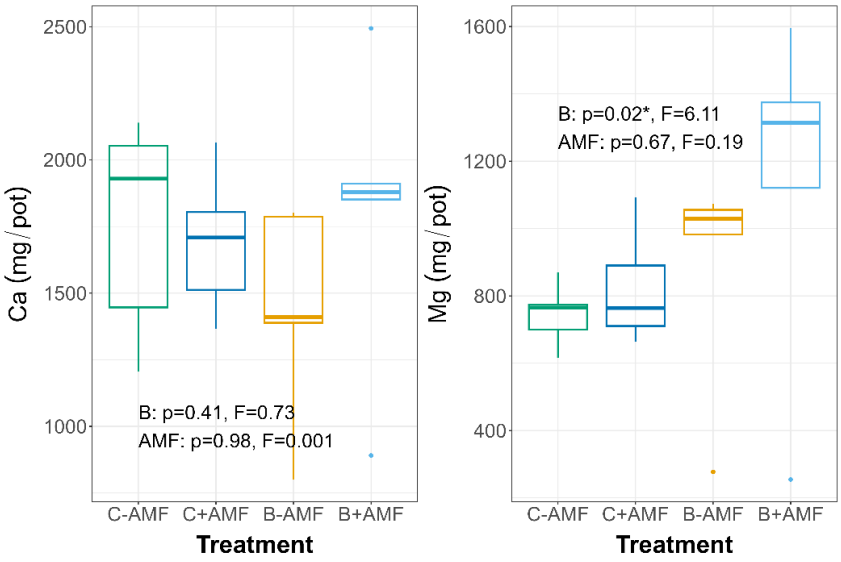


Figure S12: Ca and Mg stocks in the plant for each treatment (C-AMF, C+AMF, B-AMF, B+AMF) and mesocosm, calculated by multiplying each cation concentration in each plant tissue (corn, stem, root, leaves, tassel) by the biomass of said plant tissue and then summating the stocks in each plant tissue. Boxes represent the interquartile range (25th–75th percentile), horizontal lines indicate the median, and whiskers extend to the most extreme data points within 1.5× of the interquartile range. Points outside this range are plotted as outliers. p- and F-values are shown from an ANOVA analysis with stock as response variable and basalt (B), AMF, and their interaction as covariables. The interaction was not significant and was excluded from the model. Significant relationships are indicated by an asterisk (*).

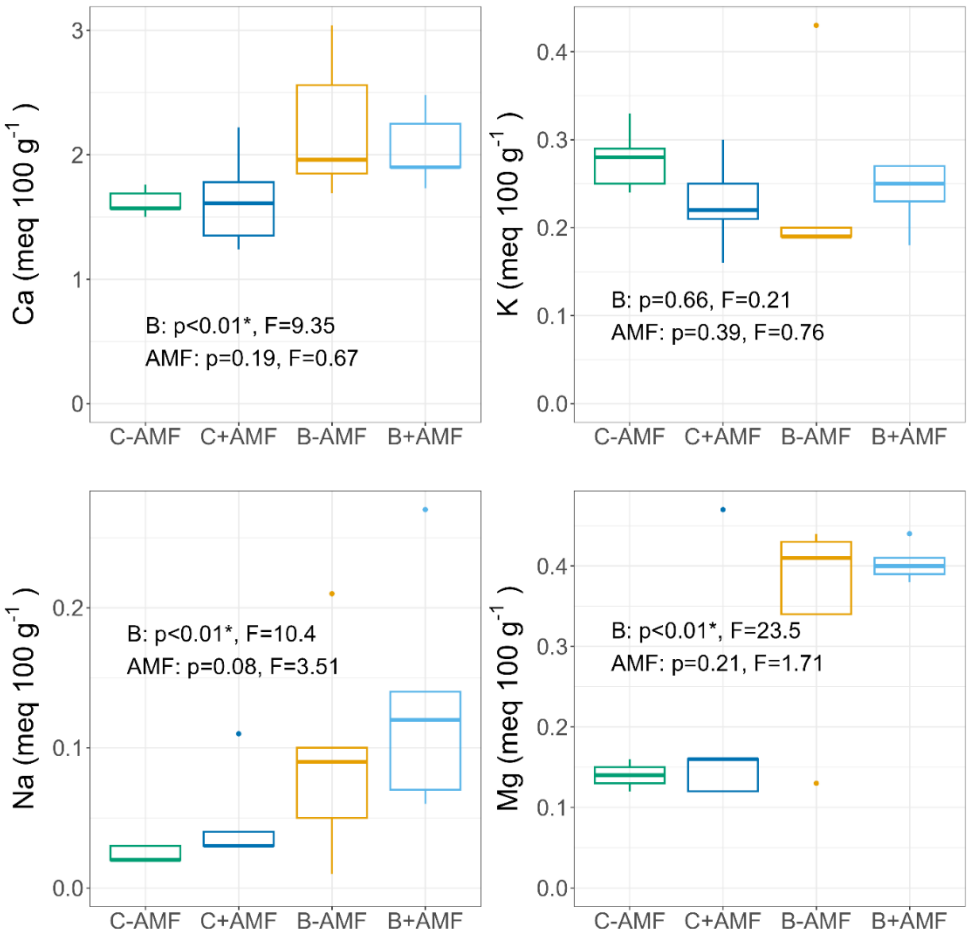


Figure S13: soil exchangeable bases (Ca, K, Mg and Na) for each treatment (B-AMF = basalt without AMF, B+AMF = basalt with AMF, CP-A = control without AMF, CP+A = control with AMF). p- and F-values are shown from an ANOVA analysis with the exchangeable bases as response variable and basalt (B), AMF and their interaction as covariables. Interactions were not significant and were excluded from the model. Significant relationships are indicated by an asterisk (*).

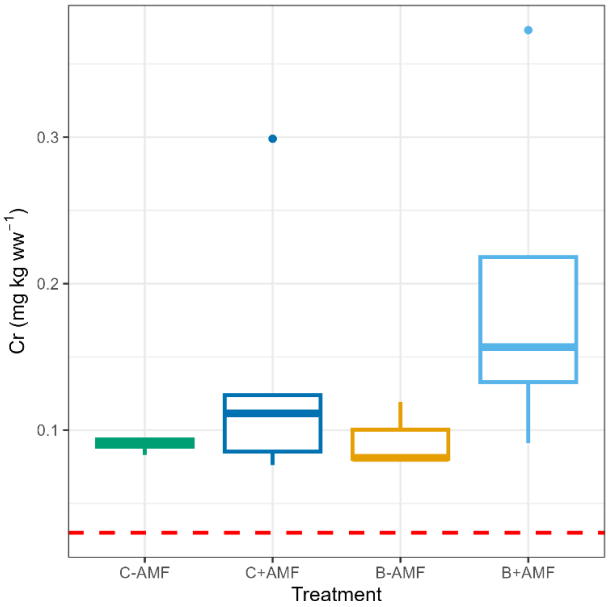


Figure S14: Concentration of Cr in the corn of *Zea mays* for each treatment (C-AMF = control without AMF, C+AMF = control with AMF, B-AMF = basalt without AMF, B+AMF = basalt with AMF) compared to World Health Organization (WHO) guidelines (dashed red line). Boxes represent the interquartile range (25th–75th percentile), horizontal lines indicate the median, and whiskers extend to the most extreme data points within 1.5× of the interquartile range. Points outside this range are plotted as outliers.

Supplementary Tables

Table S1: Soil elemental composition according to XRF. Measurements were carried out on milled samples using a WD-XRF spectrometer (Bruker S8 Tiger 4K).

Formula	Concentration (%)
SiO_2	83.13
Al_2O_3	8.70
Fe_2O_3	2.24
K_2O	1.95
Na_2O	1.09
P_2O_5	0.72
TiO_2	0.70
MgO	0.61
CaO	0.43
SO_3	0.12

Table S2: Dry weights of corn smut galls for each treatment (C-AMF = control without AMF, C+AMF = control with AMF, B-AMF = basalt without AMF, B+AMF = basalt with AMF) at the end of the experiment. p- and F-values are shown from a general linear model with gall weight as response variable and basalt, AMF and their interaction, indicated by a caret (^), as covariables. The interaction was not significant (ns) and was excluded from the model.

	Fungus dry weight (g)				**Statistical analysis**		
Replica	**B+AMF**	**B-AMF**	**C+AMF**	**C-AMF**	**Variable**	**p-value**	**F-value**
1	0	0	0	0	Basalt	0.29	1.19
2	0.27	0	0	0.06	AMF	0.93	0.05
3	0.51	0.06	0.21	0.27	Basalt ^ AMF	ns	ns
4	0.53	1.38	0.35	0.44			
5	6.89	6.96	2.05	0.67			

Table S3: p- and F-values from an ANOVA analysis with element content in four soil fractions and for three different soil layers as response variable, and basalt, AMF and their interaction as covariates. Interactions that were not significant were excluded from the model. Significant relationships are indicated in bold, while p values between 0.05 and 0.099 in italics. Whenever assumptions of normality or homoscedasticity were not met, the non-parametric Kruskal-Wallis test was used instead, with treatment as covariate. In those cases, p-and chi² values are shown. Whenever element concentrations for any fraction-layer combination were below detection or below the limit of quantification, statistical analysis was not possible.

			BASALT		**AMF**		**BASALT X AMF**	
ELEMENT	Layer	Fraction	p	F	p	F	p	F
CALCIUM (Ca)	0-20	Carbonate	0.41	0.71	0.28	1.25	ns	ns
		Exchangeable	**0.037**	**5.12**	0.72	0.14	ns	ns
		Oxidisable	0.97	0.001	*0.095*	*3.1*	ns	ns
		Reducible	Kruskal-Wallis test		p=0.49; chi²=2.45			
	20-40	Carbonate	**Kruskal-Wallis test**		**p<0.001; chi²=16.63**			
		Exchangeable	**<0.0001**	**40.77**	0.35	0.9	ns	ns
		Oxidisable	**<0.0001**	**43.63**	0.18	1.95	ns	ns
		Reducible	**Kruskal-Wallis test**		**p<0.01; chi²=14.96**			
	40-60	Carbonate	Kruskal-Wallis test		p=0.72; chi²=1.35			
		Exchangeable	0.23	1.58	0.76	0.09	ns	ns
		Oxidisable	Kruskal-Wallis test		p=0.66; chi²=1.62			
		Reducible	0.95	<0.01	0.9	0.02	ns	ns
MAGNESIUM (Mg)	0-20	Carbonate	**0.017**	**6.98**	*0.053*	*4.3*	ns	ns
		Exchangeable	**<0.01**	**11.58**	0.15	2.29	ns	ns
		Oxidisable	0.3	1.4	0.28	1.23	ns	ns
		Reducible	Kruskal-Wallis test		p=0.21; chi²=4.53		ns	ns
	20-40	Carbonate	**Kruskal-Wallis test**		**p<0.01; chi²= 16.2**			
		Exchangeable	**Kruskal-Wallis test**		**p<0.01; chi²=12.3**			
		Oxidisable	0.15	2.27	0.17	2.06	ns	ns
		Reducible	**Kruskal-Wallis test**		**p<0.01; chi²= 14.39**		ns	ns
	40-60	Carbonate	0.35	0.92	*0.07*	3.71	ns	ns
		Exchangeable	0.45	0.59	0.94	<0.01	ns	ns
		Oxidisable	0.54	0.4	0.57	0.34	ns	ns
		Reducible	0.14	2.41	0.84	0.04	ns	ns
SODIUM (Na)	0-20	Carbonate	0.6	0.28	**0.048**	**4.5**	ns	ns
		Exchangeable	**Kruskal-Wallis test**		**p=0.046; chi²=7.98**		ns	ns
		Oxidisable	0.52	0.43	0.42	0.7	ns	ns
		Reducible	**0.006**	9.4	*0.059*	*4.07*	ns	ns
	20-40	Carbonate	**Kruskal-Wallis test**		**p<0.01; chi²= 15.2**			
		Exchangeable	**<0.0001**	83.5	0.27	1.29	ns	ns
		Oxidisable			below detection			
		Reducible	**Kruskal-Wallis test**		**p<0.01; chi²= 13.8**		ns	ns
	40-60	Carbonate	0.23	1.53	0.95	<0.01	ns	ns
		Exchangeable	Kruskal-Wallis test		p=0.13; chi²=5.64		ns	ns
		Oxidisable			below detection			
		Reducible	0.55	0.37	0.92	0.01	ns	ns
POTASSIUM (K)	0-20	Carbonate	0.63	0.24	*0.08*	*3.49*	ns	ns
		Exchangeable	0.23	1.55	0.68	0.18	ns	ns
		Oxidisable	0.22	1.61	0.55	0.37	ns	ns
		Reducible	0.15	2.32	0.7	0.15	ns	ns

Table S3: continued.

			BASALT		AMF		BASALT X AMF	
ELEMENT	Layer	Fraction	p	F	p	F	p	F
POTASSIUM (K)	20-40	Carbonate	**Kruskal-Wallis test**		**p<0.001; chi²=17**			
		Exchangeable	0.15	2.27	0.31	1.08	ns	ns
		Oxidisable	below detection					
		Reducible	**0.02**	**6.57**	0.45	0.58	ns	ns
	40-60	Carbonate	below detection					
		Exchangeable	0.45	0.6	0.23	1.57	ns	ns
		Oxidisable	0.36	0.88	0.34	0.97	ns	ns
		Reducible	0.09	3.21	0.86	0.03	ns	ns
IRON (Fe)	0-20	Carbonate	0.99	<0.01	0.83	0.05	ns	ns
		Exchangeable	0.76	0.1	0.26	1.35	ns	ns
		Oxidisable	**0.03**	**5.87**	0.56	0.36	ns	ns
		Reducible	0.54	0.39	0.95	0.003	ns	ns
	20-40	Carbonate	**<0.0001**	**32.1**	0.54	0.39	ns	ns
		Exchangeable	0.29	1.18	0.82	0.05	ns	ns
		Oxidisable	*0.08*	3.4	0.27	1.31	ns	ns
		Reducible	**<0.0001**	**35.1**	0.89	0.02	ns	ns
	40-60	Carbonate	Kruskal-Wallis test		p=0.92; chi²=0.49			
		Exchangeable	below detection					
		Oxidisable	Kruskal-Wallis test		p=0.501; chi²=2.36		ns	ns
		Reducible	*0.09*	*3.18*	0.91	0.01	ns	ns
SILICON (Si)	0-20	Carbonate	Kruskal-Wallis test		p=0.29; chi²=3.76			
		Exchangeable	Kruskal-Wallis test		p=0.6; chi²=1.88			
		Oxidisable	0.2	1.79	0.44	0.62	ns	ns
		Reducible	0.43	0.66	0.28	1.22	ns	ns
	20-40	Carbonate	**Kruskal-Wallis test**		**p<0.01; chi²=15.1**			
		Exchangeable	Kruskal-Wallis test		p=0.5; chi²=2.39			
		Oxidisable	**<0.01**	**8.53**	0.56	0.36	ns	ns
		Reducible	0.22	1.62	0.27	1.26	ns	ns
	40-60	Carbonate	Kruskal-Wallis test		p=0.52; chi²=2.28			
		Exchangeable	0.15	2.31	0.13	2.57		
		Oxidisable	0.7	0.16	0.41	0.72	ns	ns
		Reducible	0.13	2.5	0.89	0.02	ns	ns
ALUMINUM (Al)	0-20	Carbonate	0.77	0.09	*0.07*	*3.81*	ns	ns
		Exchangeable	0.55	0.37	0.13	2.53	ns	ns
		Oxidisable	0.15	2.28	0.77	0.09	ns	ns
		Reducible	0.17	2.04	0.92	0.01	ns	ns
	20-40	Carbonate	**<0.0001**	**31.7**	0.14	2.42	ns	ns
		Exchangeable	0.22	1.63	0.87	0.03	ns	ns
		Oxidisable	**<0.01**	**10.13**	*0.099*	*3.04*	ns	ns
		Reducible	0.24	1.47	0.75	0.11	ns	ns
	40-60	Carbonate	Kruskal-Wallis test		p=0.79; chi²=1.04			
		Exchangeable	below detection					
		Oxidisable	Kruskal-Wallis test		p=0.5; chi²=2.36			
		Reducible	0.25	1.43	0.97	<0.01	ns	

Table S3: continued.

			BASALT		AMF		BASALT X AMF	
ELEMENT	Layer	Fraction	p	F	p	F	p	F
CROMIUM (Cr)	0-20	Carbonate	below the limit of quantification					
		Exchangeable	below the limit of quantification					
		Oxidisable	Kruskal-Wallis test		p=0.15; chi²=5.35			
		Reducible	**0.049**	**4.47**	0.41	0.71	ns	ns
	20-40	Carbonate	below the limit of quantification					
		Exchangeable						
		Oxidisable	*Kruskal-Wallis test*		*p=0.09; chi²= 6.43*			
		Reducible	0.13	2.51	*0.08*	*3.57*	ns	ns
	40-60	Carbonate	Kruskal-Wallis test		p=0.55; chi²= 2.12			
		Exchangeable	below detection					
		Oxidisable	0.36	0.87	0.48	0.54	ns	ns
		Reducible	*0.055*	*4.23*	0.8	0.07	ns	ns
NICKEL (Ni)	0-20	Carbonate	below the limit of quantification					
		Exchangeable	below the limit of quantification					
		Oxidisable	below the limit of quantification					
		Reducible	0.32	1.05	*0.09*	*3.2*	ns	ns
	20-40	Carbonate	below the limit of quantification					
		Exchangeable	below the limit of quantification					
		Oxidisable	below detection					
		Reducible	**Kruskal-Wallis test**		**p<0.01; chi² = 14.4**			
	40-60	Carbonate	Kruskal-Wallis test		p=0.55; chi² = 2.12			
		Exchangeable	below detection					
		Oxidisable	below detection					
		Reducible	0.11	2.91	0.92	0.01	ns	ns
ZINC (Zn)	0-20	Carbonate	**<0.01**	**13.93**	0.9	0.01	ns	ns
		Exchangeable	**<0.001**	**20.3**	0.51	0.46	ns	ns
		Oxidisable	Kruskal-Wallis test		p=0.55; chi² = 2.09			
		Reducible	*0.07*	*3.76*	0.46	0.57	*0.07*	3.74
	20-40	Carbonate	*Kruskal-Wallis test*		*p=0.09; chi²= 6.38*			
		Exchangeable	**Kruskal-Wallis test**		**p<0.01*; chi² =11.66**			
		Oxidisable	below detection					
		Reducible	**0.045**	**4.65**	0.65	0.22	ns	ns
	40-60	Carbonate	0.66	0.2	0.76	0.09	ns	ns
		Exchangeable	Kruskal-Wallis test		p=0.28; chi²= 3.8			
		Oxidisable	Kruskal-Wallis test		p=0.44; chi²= 2.69			
		Reducible	0.38	0.8	0.98	<0.01	ns	ns

Table S4: Direction and magnitude of the basalt effect on elements in the exchangeable, reducible and oxidizable pools of two soil layers (0-20 and 20-40 cm; elements in the 40-60 cm layer were not affected by basalt amendment in the exchangeable, reducible and oxidizable pools) at the end of the experiment. No significant effects on the oxidizable pool in the 0-20 cm layer were detected; therefore, the corresponding column has been removed. The magnitude is reported as both net basalt effect in mg kg soil^{-1}, calculated as ΔBasalt − ΔControl (where Δ = content$_{day113i,j}$ − content$_{day9i,j}$, where i = fraction considered and j = element considered, grouping the two control (C-AMF and C+AMF) and two basalt (B-AMF and B+AMF) treatments), and as percentage change relative to their initial pools (content$_{day9i,j}$; in brackets). Positive values symbolize a basalt-driven increase in elemental concentration, while negative values symbolize a decrease. Only significant effects are reported. Trends are indicated in italics. No significant AMF effect was detected. Values are reported as means ± SE for variables analysed by ANOVA and medians ± bootstrapped SE for variables analysed using the Kruskal-Wallis test (see Table S8 for statistical test results).

ELEMENT	**0-20 CM LAYER**		**20-40 CM LAYER**		
	Exchangeable	Reducible	Exchangeable	Reducible	Oxidizable
Ca	+87.5 ± 37.7 (+28.8%)		+72.6 ± 11.3 (+24.6%)	+116.0 ± 9.3 (117.5%)	+4.5 ± 0.7 (90.7%)
Mg	+11.5 ± 5.9 (35.5%)		+36.3 ± 2.0 (159.2%)	+1200.4 ± 71.6 (462.1%)	
Fe				+668.3 ± 109.2 (15.8%)	*+0.6 ± 0.3 (+57.2%)*
Na	C-AMF to B+AMF: +13.8	-30.8 ± 11.2 (-79.6%)	+20.3 ± 2.0 (+557.4%)	+72.5 ± 6.1 (+1217.8%)	
K				-39.8 ± 15.5 (-18.1%)	
Si					+27.6 ± 9.5 (8.8%)
Cr					No significant differences in pairwise comparison
Ni					
Zn	-0.4 ± 0.08 (-70.1%)		-0.5 ± 0.1 (-98.8%)		
Al					+5.1 ± 1.7 (84.7%)

Table S5: Leachate volumes during the experiment for each mesocosm. Only on two dates at the beginning of the growing season, leachates were collected. There were no leachates after 20 June 2022.

MESOCOSM	TREATMENT	DATE	VOLUME (L)
1	B+AMF	2022-06-10	1.7
		2022-06-20	0.1
5	B-AMF	2022-06-10	0.88
10	B+AMF	2022-06-10	0.39
		2022-06-20	0.16
14	B-AMF	2022-06-10	0.81
		2022-06-20	0.09
18	C+AMF	2022-06-10	0.1
22	C-AMF	2022-06-20	0.1
25	C+AMF	2022-06-10	0.52
28	C+AMF	2022-06-10	0.076
37	B-AMF	2022-06-10	0.85
		2022-06-20	0.05
42	C+AMF	2022-06-10	0.53
46	C-AMF	2022-06-10	0.79
50	B+AMF	2022-06-10	0.87
		2022-06-20	0.095
53	B+AMF	2022-06-10	0.63
		2022-06-20	0.3
56	C-AMF	2022-06-10	0.06
		2022-06-10	0.222
62	B-AMF	2022-06-10	0.7

Table S6: Number of mesocosms for which soil heavy metal contents in each depth and soil fraction combination was below detection limit (bd) or lower than the limit of quantification (<LOQ) for each treatment. The element can be detected without being quantified, therefore elemental concentrations can be higher than the detection limit but lower than the limit of quantification. The number is given compared to the total number of mesocosms of that treatment. LOQ is also given for each element. If none of the samples were bd or <LOQ, a "/" is shown, if all samples were bd or <LOQ, "all" is shown.

		Al		**Cr**		**Ni**		**Zn**	
		bd	<LOQ <187.9 ppm	bd	<LOQ <19.5 ppb	bd	<LOQ <19.4 ppb	bd	<LOQ <37.2 ppm
0-20 cm	Exchangeable	/	/	/	All	B-AMF: 2/5 B+AMF: 0/5 C-AMF: 2/5 C+AMF: 1/5	B-AMF: 3/5 B+AMF: 5/5 C-AMF: 3/5 C+AMF: 4/5	/	B-AMF: 3/5 B+AMF: 2/5 C-AMF: 1/5 C+AMF: 1/5
	Carbonate	/	/	/	All	/	All	/	/
	Oxidisable	B-AMF: 0/5 B+AMF: 1/5 C-AMF: 0/5 C+AMF: 0/5	/	/	B-AMF: 1/5 B+AMF: 2/5 C-AMF: 2/5 C+AMF: 1/5	B-AMF: 0/5 B+AMF: 0/5 C-AMF: 5/5 C+AMF: 4/5	B-AMF: 5/5 B+AMF: 5/5 C-AMF: 0/5 C+AMF: 0/5	/	B-AMF: 0/5 B+AMF: 1/5 C-AMF: 1/5 C+AMF: 0/5
	Reducible	/	/	/	/	/	/	/	/
20-40 cm	Exchangeable	/	/	/	All	B-AMF: 0/5 B+AMF: 0/5 C-AMF: 3/5 C+AMF: 3/5	B-AMF: 5/5 B+AMF: 5/5 C-AMF: 2/5 C+AMF: 2/5	/	B-AMF: 1/5 B+AMF: 1/5 C-AMF: 0/5 C+AMF: 0/5
	Carbonate	/	/	/	All	/	All	/	/
	Oxidisable	/	/	B-AMF: 0/5 B+AMF: 0/5 C-AMF: 2/5 C+AMF: 1/5	/	All	/	All	/
	Reducible	/	/	/	/	/	/	/	/
40-60 cm	Exchangeable	All	/	All	/	All	/	B-AMF: 1/5 B+AMF: 2/5 C-AMF: 1/4 C+AMF: 4/5	B-AMF: 4/5 B+AMF: 2/5 C-AMF: 3/4 C+AMF: 1/5
	Carbonate	B-AMF: 1/5 B+AMF: 1/5 C-AMF: 1/4 C+AMF: 1/5	/	B-AMF: 4/5 B+AMF: 5/5 C-AMF: 4/4 C+AMF: 4/5	/	B-AMF: 4/5 B+AMF: 5/5 C-AMF: 4/4 C+AMF: 4/5	/	B-AMF: 1/5 B+AMF: 1/5 C-AMF: 1/4 C+AMF: 0/5	/
	Oxidisable	/	B-AMF: 5/5 B+AMF: 5/5 C-AMF: 3/4 C+AMF: 4/5	/	/	/	All	B-AMF: 1/5 B+AMF: 2/5 C-AMF: 1/4 C+AMF: 3/5	B-AMF: 4/5 B+AMF: 3/5 C-AMF: 2/4 C+AMF: 1/5
	Reducible	/	/	/	/	/	/	/	/

Table S7: Heavy metals (Al, Cr, Ni, Zn) contents in the soil at the end of the experiment for the layers and fractions for which content in other mesocosms and/or treatments were all below the detection limit or lower than the limit of quantification.

MESOCOSM	FRACTION	LAYER	TREATMENT	ELEMENT	CONTENT (mg kg^{-1} soil)
18	Carbonate	40-60cm	C+AMF	Cr	0.96
18	Carbonate	40-60cm	C+AMF	Ni	0.98
22	Oxidisable	40-60cm	C-AMF	Al	45.11
22	Oxidisable	40-60cm	C-AMF	Zn	0.49
61	Oxidisable	40-60cm	C+AMF	Al	45.32
61	Oxidisable	40-60cm	C+AMF	Zn	0.55
61	Oxidisable	0-20cm	C+AMF	Ni	0.53
62	Carbonate	40-60cm	B-AMF	Cr	0.98
62	Carbonate	40-60cm	B-AMF	Ni	1.03

Table S8: Comparison of average increases (moles charge equivalents $mesocosm^{-1}$) ± SE between the start and the end of the experiment in the soil, and increases in Ca, Mg and K in the plants compared to C-AMF treatment ± SE. As leachates were absent after 20 June 2022, they were not included in weathering rates calculations.

TREATMENT	UNIT	SOIL	PLANTS
B+AMF	mol $mesocosm^{-1}$	4.12 ± 0.32	0.04 ± 0.02
B-AMF	mol $mesocosm^{-1}$	3.74 ± 0.35	0.02 ± 0.02
C+AMF	mol $mesocosm^{-1}$	0.65 ± 0.1	0.01 ± 0.02
C-AMF	mol $mesocosm^{-1}$	0.67 ± 0.13	0

Table S9: p- and F-values from an ANOVA analysis with element concentrations in various plant parts as response variable, and basalt, AMF and their interaction as covariables. Interactions that were not significant were excluded from the model. Significant relationships are indicated by an asterisk (*). Assumptions of normality or heteroscedasticity were not met for stem and corn C contents. In those instances, a non-parametric Kruskal-Wallis test was used instead, with treatment as a covariable. p-and F-values or p- and chi²- values are shown. Cd, Cr, and V concentrations in the leaves, and V concentrations in corn were all below the limit of quantification (<LOQ). Despite the significant basalt x AMF interaction in stem C:N ratio, the Tukey post-hoc pairwise comparison revealed no significant difference.

		Stem		**Leaves**		**Corn**		**Tassel**		**Roots**	
		p-value	F	p-value	F	p-value	F	p-value	F	p-value	F
Al	Basalt	0.62	0.25	0.23	1.58	0.23	1.56	0.69	0.16	0.62	0.25
	AMF	0.34	0.96	0.23	1.52	0.38	0.84	0.44	0.64	0.66	0.19
Ca	Basalt	0.95	<0.01	0.5	0.48	0.19	1.94	0.99	0	0.53	0.41
	AMF	0.94	<0.01	0.83	0.05	0.25	1.42	0.28	1.23	0.13	2.56
Cd	Basalt	0.42	0.69	<LOQ		0.25	1.47	0.74	0.11	0.61	0.27
	AMF	**<0.01***	10.1			0.42	0.7	0.47	0.55	0.66	0.20
Cr	Basalt	0.92	0.01	<LOQ		0.35	0.93	0.19	0.86	0.49	0.5
	AMF	0.99	<0.01			**0.03***	5.68	0.51	0.46	0.87	0.03
Fe	Basalt	0.34	0.97	0.21	1.69	0.65	0.22	0.41	0.7	0.49	0.5
	AMF	0.33	0.99	0.49	0.5	0.83	0.05	0.9	0.02	0.8	0.07
K	Basalt	0.27	1.32	**0.03***	5.51	0.23	1.54	0.84	0.04	0.96	0.03
	AMF	0.38	0.81	0.74	0.12	0.41	0.70	0.81	0.06	0.62	0.26
Mg	Basalt	**<0.01***	14.7	**<0.001***	19.02	0.26	1.39	**<0.01***	12.59	**<0.001***	36.3
	AMF	0.88	0.02	0.32	1.07	0.47	0.55	0.06	4.18	**<0.01***	11.6
	B^AMF	ns	ns	ns	ns	ns	ns	ns	ns	*0.08*	3.47
Ni	Basalt	0.58	0.31	0.1	3.01	**0.02***	7.21	0.09	3.19	0.69	0.17
	AMF	0.99	0	0.97	<0.01	**0.03***	5.63	0.37	0.86	0.94	<0.01
P	Basalt	0.89	0.02	0.75	0.11	0.90	0.2	0.37	0.84	0.34	0.94
	AMF	0.20	1.79	**0.04***	5.2	0.21	1.74	0.38	0.83	0.21	1.73
Pb	Basalt	0.11	2.87	**0.03***	5.36	0.67	0.19	0.37	0.86	**<0.01***	14.9
	AMF	0.52	0.43	0.68	0.17	0.62	0.26	0.91	0.01	0.48	0.52
	B^AMF	ns	ns	ns	ns	ns	ns	ns	ns	**0.048***	4.63
V	Basalt	0.95	<0.01	<LOQ		<LOQ		0.59	0.3	0.35	0.93
	AMF	0.24	1.5					0.86	0.03	*0.09*	3.19
	B^AMF	ns	ns					ns	ns	*0.054*	4.36
Zn	Basalt	0.75	0.1	0.62	0.25	0.15	2.27	0.75	0.1	0.36	0.89
	AMF	0.53	0.4	0.58	0.31	0.63	0.25	0.21	1.74	0.28	1.24
C	Basalt	Kruskal-Wallis test:		**0.02***	6.87	Kruskal-Wallis test:		Kruskal-Wallis test:		0.46	0.57
	AMF	P=0.50	chi²= 2.35	0.19	1.85	p=0.87, chi²=0.73		p=0.31, chi²=3.57		0.66	0.20
N	Basalt	0.57	0.33	0.16	2.15	0.86	0.03	0.84	0.04	0.61	0.27
	AMF	0.52	0.44	0.12	2.76	0.62	0.26	*0.05*	4.34	*0.09*	3.16
Si	Basalt	**<0.01***	9.08	0.19	1.83	0.14	2.41	**0.02***	6.9	0.34	0.98
	AMF	0.63	0.24	0.60	0.28	0.88	0.03	0.47	0.55	0.41	0.72
CN ratio	Basalt	0.45	0.61	0.17	2.01	0.9	0.02	0.98	0.0006	0.88	0.03
	AMF	0.5	0.47	0.22	1.60	0.55	0.37	**0.02***	6.21	*0.09*	3.23
	B^AMF	**0.047***	4.62	ns	ns	ns	ns	ns	ns	ns	ns

References

Gislason, S. R. and Oelkers, E. H.: Mechanism, rates, and consequences of basaltic glass dissolution: II. An experimental study of the dissolution rates of basaltic glass as a function of pH and temperature, Geochimica et Cosmochimica Acta, 67, 3817-3832, 10.1016/s0016-7037(03)00176-5, 2003.
Palandri, J. L. and Kharaka, Y. K.: A compilation of rate parameters of water-mineral interaction kinetics for application to geochemical modeling, US Geological Survey2331-1258, 2004.
Ven, A., Verlinden, M. S., Verbruggen, E., Vicca, S., and Hart, M.: Experimental evidence that phosphorus fertilization and arbuscular mycorrhizal symbiosis can reduce the carbon cost of phosphorus uptake, Funct Ecol, 33, 2215-2225, 10.1111/1365-2435.13452, 2019.